Cell

# Identification of a Bacterial Type III Effector Family with G Protein Mimicry Functions

Neal M. Alto,[1,2] Feng Shao,[3] Cheri S. Lazar,[1,2] Renee L. Brost,[4,5] Gordon Chua,[4,5] Seema Mattoo,[1,2] Stephen A. McMahon,[6] Partho Ghosh,[1,2] Timothy R. Hughes,[4,5] Charles Boone,[4,5] and Jack E. Dixon[1,2,*]
[1] Department of Pharmacology, Cellular and Molecular Medicine
[2] Department of Chemistry and Biochemistry
University of California, San Diego, La Jolla, CA 92093, USA
[3] National Institute of Biological Sciences, Beijing, 102206, China
[4] Banting and Best Department of Medical Research
[5] Department of Medical Genetics and Microbiology
University of Toronto, Toronto, Ontario, Canada
[6] Centre for Biomolecular Sciences, The University of St Andrews, Fife KY16 9ST, United Kingdom
*Contact: jedixon@ucsd.edu
DOI 10.1016/j.cell.2005.10.031

## SUMMARY

**Many bacterial pathogens use the type III secretion system to inject "effector" proteins into host cells. Here, we report the identification of a 24 member effector protein family found in pathogens including *Salmonella*, *Shigella*, and enteropathogenic *E. coli*. Members of this family subvert host cell function by mimicking the signaling properties of Ras-like GTPases. The effector IpgB2 stimulates cellular responses analogous to GTP-active RhoA, whereas IpgB1 and Map function as the active forms of Rac1 and Cdc42, respectively. These effectors do not bind guanine nucleotides or have sequences corresponding the conserved GTPase domain, suggesting that they are functional but not structural mimics. However, several of these effectors harbor intracellular targeting sequences that contribute to their signaling specificities. The activities of IpgB2, IpgB1, and Map are dependent on an invariant WxxxE motif found in numerous effectors leading to the speculation that they all function by a similar molecular mechanism.**

## INTRODUCTION

*Salmonella typhi*, *Shigella flexneri*, and enteropathogenic *Escherichia coli* (EPEC) are gram-negative etiological agents of typhoid fever, bacillary dysentery, and gastroenteritis in humans. Virulence associated with these enteric bacteria often correlates with the presence of a functional type III secretion system (TTSS) that acts as a conduit for delivery of bacterial "effector" proteins directly into host cells (Cornelis and Van Gijsegem, 2000; Galan and Collmer, 1999). These secreted effectors allow pathogens to limit antibacterial host immune responses or generate a cellular architecture that is advantageous to bacterial replication and disease progression. EPEC, a member of the attaching and effacing (A/E) pathogen group, intimately attaches to the apical surface of gut epithelia and destroys tight junction barrier functions through the coordinated activities of at least six type III effectors (Tir, Map, EspF, EspG, EspH, and EspI; Dean et al., 2005). Unlike EPEC however, *Salmonella* and *Shigella* are intracellular pathogens that orchestrate hosT cell invasion and cellular survival in gut epithelia and immune cells. Each of these pathogens secretes a distinct set of effector proteins that propagate their complex intracellular life cycles (Cossart and Sansonetti, 2004).

Because of their ubiquitous role in cell biology, Ras-like small G proteins are a common target for virulence factors secreted by bacterial pathogens (Boquet, 2000). There are well over 100 eukaryotic small G proteins that regulate a myriad of cellular processes including growth, differentiation, membrane trafficking, cytoskeletal organization, and nuclear import. Several key features of small G proteins allow them to perform these essential functions. First, they act as molecular switches cycling between GTP bound (active) and GDP bound (inactive) conformations. Second, most small G proteins are posttranslationally modified; the addition of isoprenoid lipid moieties allows them to associate with specific subcellular compartments. Third, they transmit signaling events in a GTP-dependent manner by activating and/or recruiting downstream target proteins to their sites of action. Previous studies have identified *Salmonella* type III bacterial effectors that function to regulate the cycling of the

nucleotides bound to the GTPases by mimicking eukaryotic GTPase-activating proteins (GAPs) and guanine nucleotide exchange factors (GEFs; Stebbins and Galan, 2001). However, there are no small G proteins encoded by enteric pathogen genomes.

Our interests in the mechanisms of host-pathogen interactions led us to identify a 24 member protein family that shares sequence similarities to the *E. coli* type III effector protein Map. Recent reports demonstrate that Map can induce hosT cell actin dynamics and disrupts tight-junction barrier function when delivered by the TTSS (Dean and Kenny, 2004; Kenny et al., 2002). Furthermore, Map is conserved throughout the A/E pathogens including enterohaemorrhagic *E. coli* (EHEC) and *Citrobacter rodentium*, suggesting that it plays an important role in pathogenesis. While the molecular mechanisms utilized by Map remain undefined, Δ*map* strains of *C. rodentium* are attenuated for virulence and display colonization defects (Mundy et al., 2004). Interestingly, we have uncovered a number of Map homologs including SifA and SifB found in *Salmonella* and IpgB1 and IpgB2 found in *Shigella*. In contrast to the pathogenic function of Map described above, SifA promotes intracellular survival and replication by maintaining the integrity of the *Salmonella*-containing vacuole (SCV; Beuzon et al., 2000). Likewise, IpgB1 participates in *Shigella* invasion by regulating actin cytoskeleton dynamics (Ohya et al., 2005). Because these biologically diverse virulence factors are related by primary sequence, it stands to reason that they all share a common unidentified biochemical activity to promote bacterial pathogenesis.

In this report, we determine the biological function of three of our 24-member effector protein family, namely IpgB1 and IpgB2 from *Shigella* as well as Map from EHEC. As suggested by their sequence relatedness, these three effectors function in a similar manner by mimicking the GTP-active form of Rho-family GTPases. Although these bacterial proteins lack many of the biochemical attributes of GTPases, they induce actin cytoskeletal dynamics in the host cell by stimulating common signaling pathways. Moreover, the signaling specificities of these type III effector proteins are governed in part by eukaryotic-like targeting motifs such as PDZ ligands and CaaX-like sequences at the C terminus. Our results suggest that direct GTPase mimicry and subcellular targeting of effectors may be a widely used mechanism in bacteria-host interactions.

## RESULTS

### Identification of Bacterial Effector Proteins with a Shared WxxxE Motif

We performed BLAST database searches starting with the EHEC effector Map as the index protein. This initial screen revealed a small number of protein homologs mostly found in the A/E pathogen group. Each member of this family shared a common Trp-x-x-x-Glu (WxxxE) motif. Next, we manually searched our BLAST results for WxxxE-containing proteins that fell below the significance threshold. By including these ''outliers'' in multiple PSI-BLAST iterations, we identified 24 distinct open reading frames that can be subdivided into at least six homolog classes including Map, TrcA, IpgB1, IpgB2, SifA, and SifB (Figure 1A). Although these putative effectors share clear regions of sequence similarity (see Figure S1 in the Supplemental Data available with this article online), the entire family has only two invariant amino acids, the Trp and Glu found in the WxxxE signature motif (Figure 1A, red residues). Secondary structure analysis predicts that each family member is composed of 6 to 8 α helices that are aligned to well-defined protein sequence boundaries, suggesting that they could have a common protein fold (Figure S1).

### IpgB2 Induces Rho-Independent Actin Stress Fibers' Assembly

An N-terminal GFP fusion of *Shigella* IpgB2 induced the formation of new actin stress fibers upon transfection of HEK293A cells (Figure 1B), HeLa, and Cos-7 cells (data not shown). No stress fibers were apparent in cells expressing only GFP (Figure 1C). Quantification of these results are shown in Figure 1F. It seemed likely that the invariant Trp or Glu residues of the WxxxE motif would be important for IpgB2 activity. As predicted, neither the $Trp^{62} \rightarrow Ala$ (Figure 1D) nor $Glu^{66} \rightarrow Ala$ (Figure 1E) mutants induced actin stress fibers. Mutations in the conserved residues $Ser^{72}$ and $Gln^{76}$ had no effect on the activity of IpgB2 under these experimental conditions (Figure 1F).

Activation of the small G protein RhoA induces actin stress fiber assembly in cells (Ridley and Hall, 1992). To test if IpgB2 is epistatic to RhoA, various inhibitors were used to disrupt signaling through Rho proteins. The C3-botulinum toxin was used to irreversibly inhibit RhoA–C (Aktories et al., 2004). Surprisingly, IpgB2 induced new actin stress fibers in the presence of the C3-exoenzyme at the same rate as IpgB2 alone (Figures 2A and 2B). In contrast, C3 abolished exogenous RhoA-induced stress fiber formation, and severe retraction fibers were found in these cells (Figures 2C and 2D). To further explore this observation, we performed additional inhibitor studies. Mutant RhoN19 was used to competitively inhibit Rho guanine-nucleotide exchange factors (GEFs) in vivo (Ridley and Hall, 1992). In addition, YopT (Iriarte and Cornelis, 1998), a *Yersinia* type III effector, was used to irreversibly block all Rho-family GTPases including Rho, Rac, and Cdc42 (Figure 2E; Shao et al., 2002). Neither RhoN19 nor YopT inhibited IpgB2 induced stress fiber formation (Figure 2F, gray bars), whereas they were both potent antagonists of exogenous RhoA (Figure 2F, black bars). These inhibitor studies demonstrate that IpgB2 induces actin stress fiber assembly through a novel mechanism that is independent of any Rho GTPase activity.

We attempted yeast two-hybrid screens with IpgB2, but yeast transformants could not be recovered. Therefore, the readily transformable IpgB2-E66A mutant was used to screen a 9.5/10.5-day-old mouse embryo library. We identified three identical clones corresponding to residues 1157–1329 of Citron kinase (CRIK), a Rho-kinase family member (Figure 3A). These residues encompass the well-defined

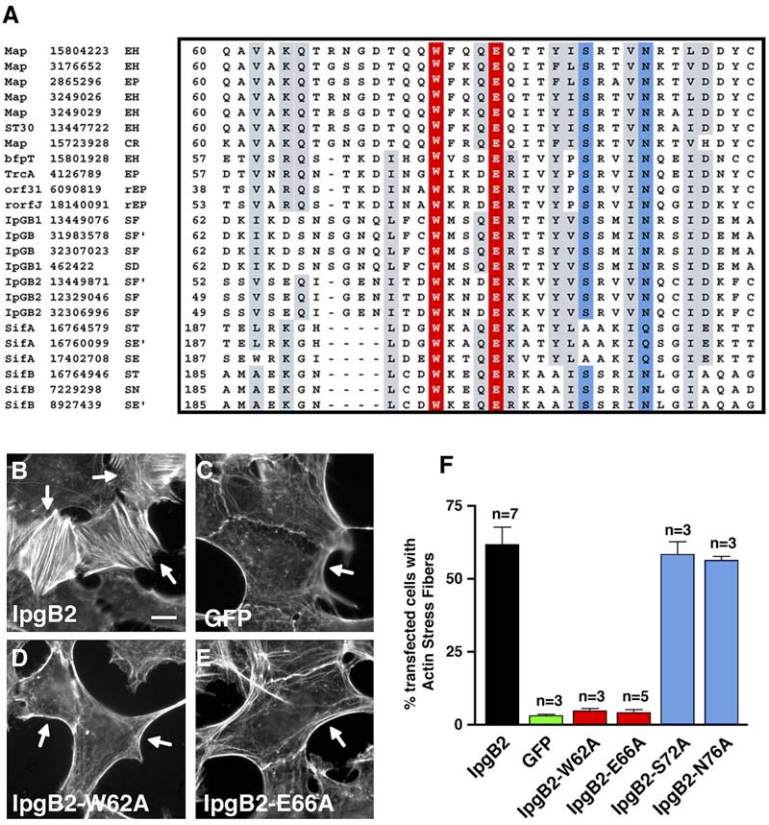


**Figure 1. Identification of the WxxxE Family of Bacterial Effectors**

(A) Clustal alignment comparing the WxxxE region of EHEC Map and 23 other family members. Genbank ID# is listed. Invariant residues are highlighted in red; residues with similar chemical properties are in gray. Nonspecific residues mutated in mammalian and yeast experiments are shown in blue. Bacterial species are as follows: enterohemorrhagic *E. coli* (EH), enteropathogenic *E. coli* (EP), *Citrobacter rodentium* (CR), rabbit enteropathogenic *E. coli* (rEP) *Shigella flexneri* (SF), *Shigella flexneri* 2A (SF′), *Shigella dysenteriae* (SD) *Salmonella typhimurium* (ST), *Salmonella enterica* (SE), *Salmonella enterica* serovar typhi (SE′), and *Salmonella enteritidis* (SN).

(B–E) Immunofluorescence microscopy of HEK293A cells transfected with GFP-IpgB2 (B), GFP (C), GFP-IpgB2-W62A (D), and GFP-IpgB2-E66A (E) and stained with rhodamine phalloidin to detect actin. Arrows indicate transfected cells. Scale bar, 15 μm.

(F) Quantification of actin stress fiber assembly in HEK293A cells transfected with IpgB2 and the indicated point mutants. One hundred fifty transfected cells were counted in at least three independent experiments. Data are presented as mean ±SEM.

Rho binding domain (GBD) of CRIK (Madaule et al., 1995). CRIK 1157–1329 interacted with both IpgB2-E66A and the active mutant of RhoA (RhoL63) in a yeast two-hybrid assay (Figure 3B). Interestingly, the GBD of CRIK is homologous to the GBD of both ROCKI and ROCKII (Figure 3A), two kinases that are required for actin stress fiber formation (Amano et al., 1997).

Both endogenous ROCKI and ROCKII were coimmunoprecipitated with GFP-IpgB2 but not with control whole-mouse IgG (Figure 3C). In vitro kinase assays were used to confirm these protein interactions. GFP-IpgB2 was immune-isolated from HEK293A cells and added to an in vitro kinase activity assay. Proteins associated with the GFP-IpgB2 immune complex had significant kinase activity directed toward the S6 substrate peptide (Figure 3D, circles). We identified the IpgB2-associated kinase as ROCK since addition of Y27632, a potent ROCK inhibitor, abolished substrate phosphorylation (Figure 3D, triangles). In control experiments, immune-isolated GFP-Map, a homolog of IpgB2 that also posses a WxxxE motif, had no associated ROCK kinase activity (Figure 3D, squares). Thus, unidentified residues or sequences outside the WxxxE motif are likely to contribute to IpgB2 substrate binding and specificity in vivo. Consistent with our protein-interaction studies, cells transfected with IpgB2 could not form actin stress fibers upon application of the ROCK inhibitor Y27632 (Figure 3E). These data further implicate ROCK as a critical target of IpgB2 during stress fiber formation.

It is well established that RhoA induces stress fiber assembly by stimulating the mammalian homolog of Diaphanous (mDia1; Watanabe et al., 1999). mDia1 is composed of an N-terminal Rho binding sequence (GBD) followed by the Formin homology domains 1 and 2 (Figure 3F). IpgB2 specifically interacted with full-length mDia1 and residues 1–301 encompassing the GBD region (Figure 3G). This data was confirmed in reciprocal coimmunoprecipitation experiments (Figure 3H). The WxxxE family member Map did not bind to any fragment of mDia1, demonstrating the specificity of these interactions (Figure 3G). Taken together, our results suggest the possibility that IpgB2 activates Rho GTPase signaling pathways by interacting with Rho ligands via the GBD domain.

## IpgB2 Activates the Rho1p GTPase Signaling Pathway in Yeast

Our yeast two-hybrid studies suggested that wild-type IpgB2 is toxic to yeast. We expressed IpgB2 driven off the *GAL1* galactose-inducible promoter and scored yeast growth when plated on galactose medium. As seen in Figure 4A, expression of IpgB2 with galactose inhibited yeast growth, whereas repression of IpgB2 allowed growth. Mutations $Trp^{62} \rightarrow Ala$ and $Glu^{66} \rightarrow Ala$ in the WxxxE motif abolished IpgB2 yeast toxicity. In contrast, substitutions at conserved (but not invariant) residues had no effect on IpgB2 toxicity in yeast (Figure 4A).

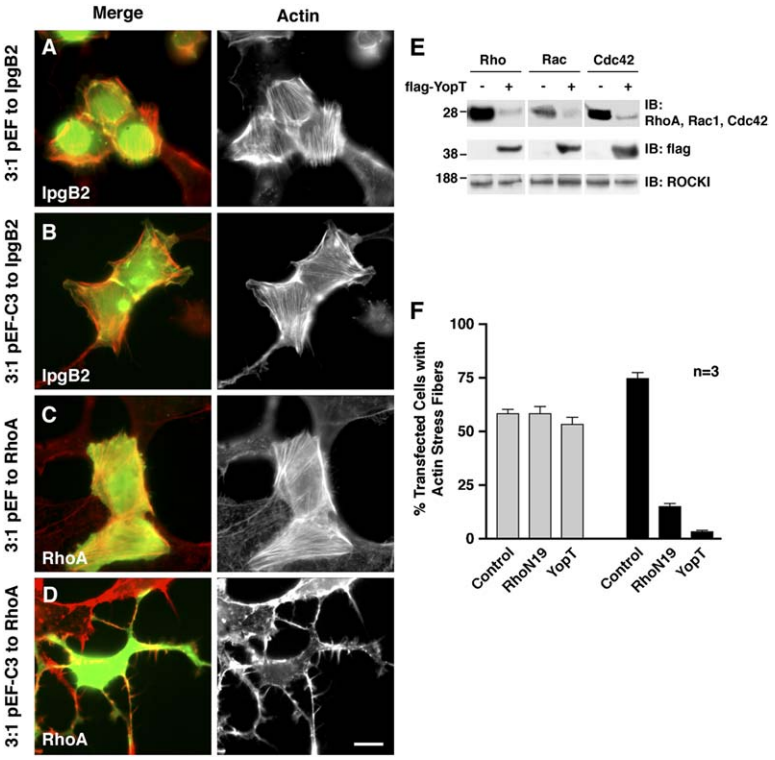


**Figure 2. IpgB2 Induces Rho-Independent Actin Stress Fibers**

(A–D) HEK293A cells cotransfected with either 0.5 μg of GFP-IpgB2 or HA-RhoA and 3-fold excess (1.5 μg) pEF control vector or pEF-C3-exoenzyme as indicated to the left of each image. Merged image of IpgB2 or RhoA (green) and actin (red) in left panel and actin morphology is shown in the right panel. Scale bar, 15 μm.

(E) YopT cleaves RhoA, Rac1, and Cdc42 from membranes in HEK293A cells. Membrane fractions (Shao et al., 2002) were probed by Western blot with the indicated antibodies (top panel) in the presence of transfected YopT (middle panel). Cellular ROCK is shown as a loading control (bottom panel).

(F) GFP-IpgB2 (gray bars) or HA-RhoA (black bars) transfected cells were scored for stress fiber formation in the presence 3-fold excess of RhoN19 or YopT cDNA. 150 transfected cells were scored in at least 3 independent experiments. Data are presented as mean ±SEM.

To gain additional insights into the mechanism of IpgB2 yeast toxicity, we designed a genetic screening strategy modeled after the synthetic genetic array (SGA); Tong et al., 2001). We refer to this technique as a pathogenic genetic array (PGA) because it allows an ordered array of ~5000 viable yeast-deletion mutants to be assayed for growth defects associated with conditional expression of any pathogen protein. We introduced *GAL1-IpgB2* into ~5000 viable gene-deletion mutants and examined their growth rates on medium containing galactose (Figure 4B). Since expression of IpgB2 is toxic to wild-type yeast, any gene-deletion mutant that grows should identify the corresponding gene as a potential target for IpgB2-induced toxicity. Out of the ~5000 strains tested, only gene deletion in *BCK1*, *SLT2*, and *RLM1* resulted in a robust growth phenotype. Remarkably, each of these genes encodes components of the cell-wall integrity Rho1p/MAP kinase (MAPK) signaling module (Heinisch et al., 1999) illustrated in Figure 4C. It is notable that PKC1 was not in our gene-deletion library because it has severe growth defects (Figure 4C). In addition, we did not isolate either MKK1 or MKK2 because these genes are functionally redundant. While yeast carrying deletions in *BCK1*, *SLT2*, and *RLM1* grow well in the presence of IpgB2, deletion of genes encoding components of other MAPK signaling modules continue to result in cell toxicity (Figure 4D). Thus, our PGA screen results are consistent with IpgB2 specifically subverting the Rho1p signaling pathway.

To test if IpgB2 signaling compares to Rho1p in yeast, we performed DNA microarray mRNA profiling because overexpression of activated Rho1p (Q68H) has a distinct and reproducible transcriptional profile (Roberts et al., 2000) and because this is an unbiased method that may determine other potential IpgB2 functions. DNA microarray analysis of ~6000 genes revealed that IpgB2 regulated 351 transcripts at a 99% confidence level (Figure 4E). The overall IpgB2 transcriptional profile strongly correlates with that of Rho1p-Q68H ($p = 0.632$), a value that resembles the correlation values derived when comparing Rho1p-Q68H to its downstream target Pkc1p-R398A ($p = 0.709$). In contrast, the IpgB2 profile did not correlate with the profile resulting from activation of the Cdc42 pheromone response MAPK cascade induced by overexpression of Ste4p ($p = 0.045$; Figure 4E; Whiteway et al., 1990). Consistent with our PGA screen, the 20 Rlm1p-regulated transcripts (Jung and Levin, 1999) were induced, suggesting that this transcription factor is indeed activated by IpgB2 (Figure 4F). Therefore, two independent genome-screening procedures support the contention that IpgB2 stimulates small G protein signaling events in a similar manner as GTP bound Rho1p.

## WxxxE Family Members Stimulate Distinct Small G Protein Signaling Events

We screened additional WxxxE bacterial effectors shown in Figure 1A for the ability to induce actin cytoskeletal dynamics. Transfection of *E. coli* Map induced cell-surface filopodia in HEK293A cells (Figure 5A), HeLa, and MDCK cells (not shown). While filopodia formation was the strongest phenotype, lamellipodia extended from the base of the actin projections (Figure 5A, enlargement). Cells expressing the following mutations in Map, $W^{74} \rightarrow A$ (data not shown) and

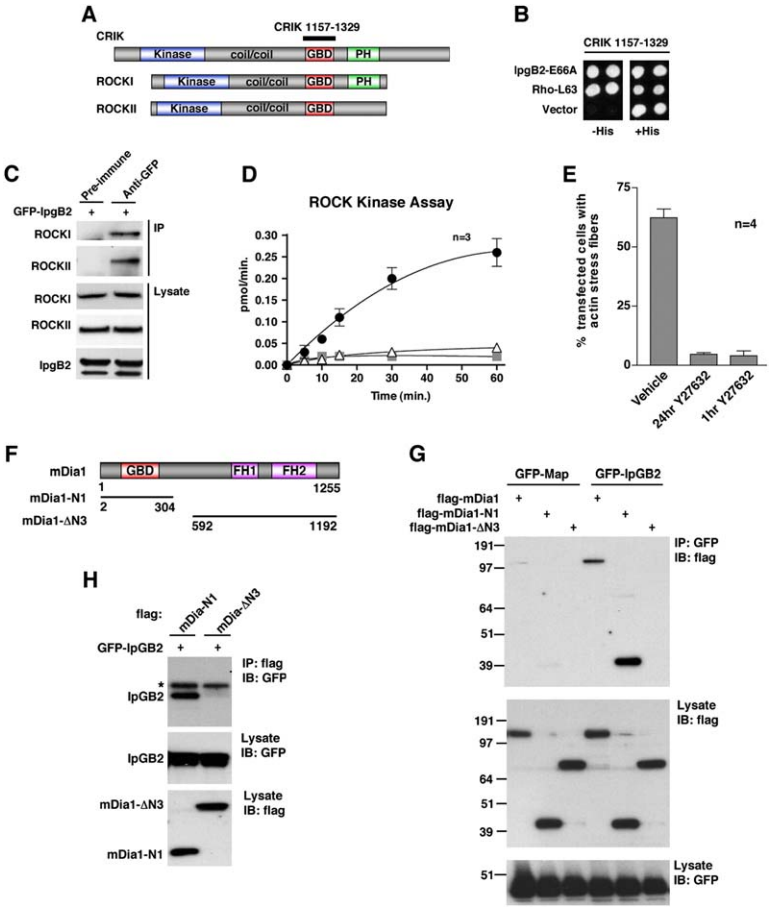


**Figure 3. IpgB2 Binds to ROCK and mDia1 in Cells**

(A) Schematic of the Rho-kinase family. Conserved domains include the kinase domain, coil/coil, GBD, and Pleckstrin homology domain (PH). The position of CRIK 1157–1329 is indicated.

(B) Interaction between residues 1157–1329 of CRIK and IpgB2-E66A or Rho-L63 were assessed by activation of the His reporter gene in yeast two-hybrid experiments (left panel). Control histidine supplemented plates are shown in the right panel.

(C) GFP-IpgB2 transfected cells were immunoprecipitated (IP) with whole mouse IgG (left lanes) or anti-GFP monoclonal antibody (right lanes). Immunoprecipitated samples (IP) or whole-cell lysates (Lysate) were immunoblotted for ROCKI, ROCKII, or GFP.

(D) ROCK kinase assay was performed on immunoprecipitated GFP-IpgB2 (circles) or GFP-Map (squares). GFP-IpgB2 samples with 10 μM Y27632 are indicated (triangles). Data is presented as pmol phosphate incorporated into the S6 peptide per minute. The average of three independent experiments and data are presented as mean ±SEM.

(E) HEK293A cells were transfected with IpgB2 and treated with vehicle alone or with 10 μM Y27632 at the time of transfection (24 hr) or 1 hr prior to cell fixation (1 hr). At least 150 cells were counted in at least three independent experiments. Data are presented as mean ±SEM.

(F) Diagram of mDia1 and truncation mutants used in this study. The GBD and Formin homology domains 1 and 2 (FH1 and FH2) are indicated.

(G) HEK293A cells were cotransfected with GFP-Map or GFP-IpgB2 and the indicated FLAG-mDia1 plasmids. Anti-GFP immunoprecipitations (IP) were probed by flag immunoblot (IB) (upper panel). Cell lysates were probed by FLAG or GFP immunoblot to show input levels (lower two panels).

(H) HEK293A cells were cotransfected with the indicated plasmids. FLAG-mDia1 constructs were immunoprecipitated (IP) with flag antibodies and probed by anti-GFP immunoblot (IB). Inputs were detected by GFP or FLAG immunoblots (lower two panels). *Cross-reacting band.

$E^{78} \rightarrow A$ (Figure 5B), were indistinguishable from GFP-transfected cells (Figure 5C). Quantification of these results are shown in Figure 5D. Notably, filopodia formation is a hallmark of signaling by the small G protein Cdc42 (Nobes and Hall, 1995).

Transfection of *Shigella* IpgB1 stimulated actin-rich membrane ruffles at the dorsal cell surface of HeLa cells (Figure 5E) and HEK293A and Cos-7 cells (data not shown). Dorsal ruffles were absent in mutant IpgB1 $E^{80} \rightarrow A$ (Figure 5F) or flag vector-expressing cells (Figure 5G). Quantification of these results are shown in Figure 5H. Notably, the dorsal actin ruffles shown in Figure 5E closely resemble those formed by the small G protein Rac1 (Nobes and Hall, 1995).

Next, we focused on the signaling properties of Map. It is well established that Cdc42 and Rac1 stimulate the Jun kinase (JNK) signal transduction cascade. JNK activity can be monitored by its phosphorylation state using phospho-specific antibodies. Both JNK and its downstream target c-*jun* were hyperphosphorylated in Map-transfected cells but not in Map-E78A-transfected cells (Figure 5I). In control experiments, the p42/44 MAP kinase (MAPK 1/2) was not phosphorylated under these conditions, demonstrating that Map specifically activates the JNK signal transduction pathway.

We conducted a series of inhibitor studies to determine if Map is epistatic to Rac1 or Cdc42 (Figure 5J). Neither

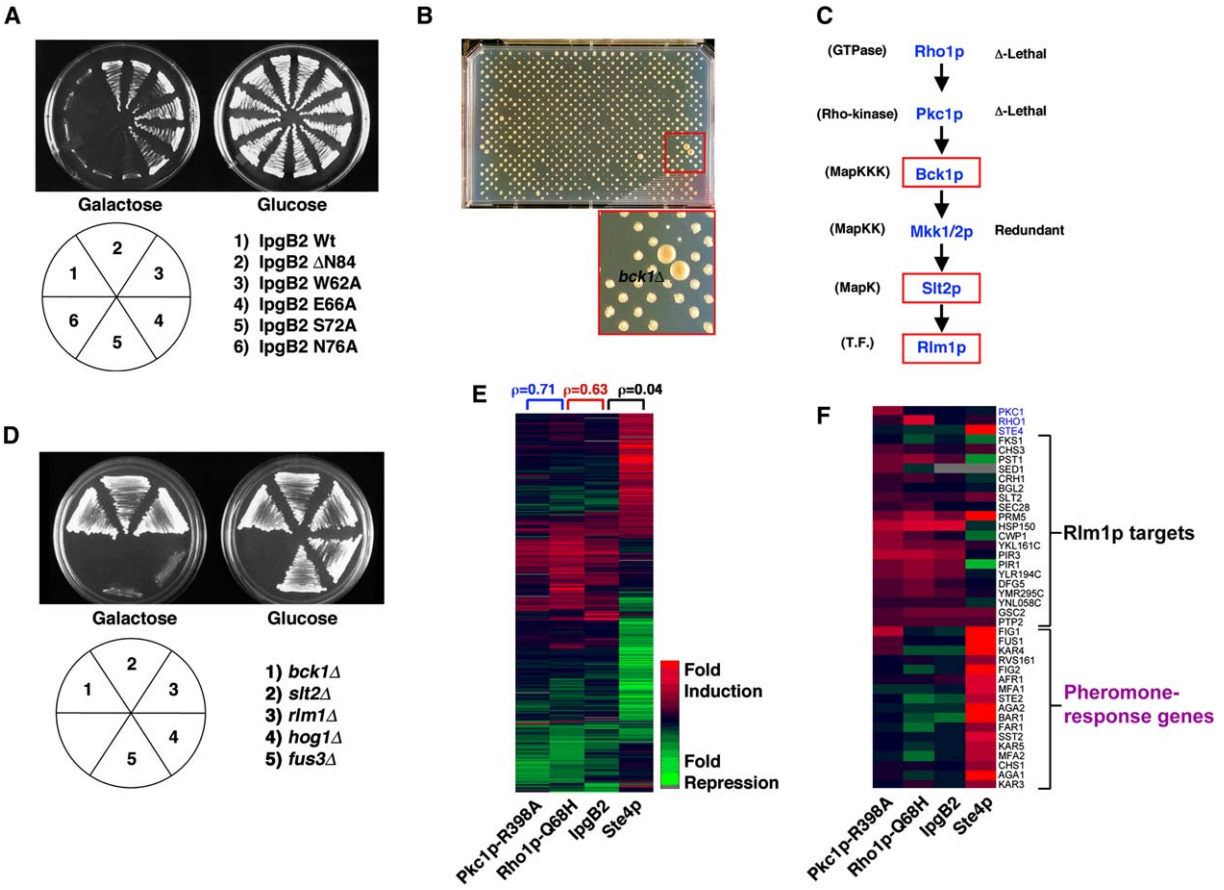


**Figure 4. IpgB2 Induces Signaling in Parallel to Rho1p in Yeast**

(A) Yeast transformed with *GAL1-IpgB2* or the indicated point mutations were streaked on galactose or glucose containing minimal medium. Experiments were performed in duplicate.

(B) Pathogenic genetic array. An example of a single 24 × 16 array plate carrying ~348 individual gene-deletion yeast strains that express *GAL1-IpgB2* (out of 16 plates and ~5000 strains). All deletion strains were plated in duplicate (diagonal) and spotted to galactose containing minimal medium. The duplicate *bck1*Δ yeast strains expressing *GAL1-IpgB2* is shown (enlarged image).

(C) Diagram of the Rho1p-activated Pkc1p/MAPK module. Function of each protein is in parenthesis (T.F. denotes transcription factor). Gene deletions that allow IpgB2 expressing yeast to survive are boxed in red.

(D) The indicated gene-deletion mutant strains carrying *GAL1-IpgB2* were each tested for colony formation on galactose medium. Growth phenotypes on glucose are shown. *fus3* and *hog1* are homologous genes of the MAPK *slt2*.

(E and F) Transcription response signatures of genes whose expression was induced (red) or repressed (green) by expression of *PKC1-R398A, Rho1p-Q68H, IpgB2, and Ste4p* for 3 hr are shown. Pearson correlations are indicated above (E). RLM1p target genes and pheromone response genes are indicated (F).

inhibition of cellular GEFs with RacN17 and Cdc42N17 or direct inhibition of Rac1 and Cdc42 by YopT proteolysis could abrogate Map-induced actin reorganization (Figure 5K). Both Rac1 and Cdc42 induce F actin nucleation by indirectly stimulating the Arp2/3 complex via the Wiskott Aldrich Syndrome protein (Wasp/Wave) family (Machesky and Insall, 1998). The C-terminal verpolin-cofilin-acidic (VCA) fragment of Wasp/Wave can inhibit Arp2/3-mediated events (Machesky and Insall, 1998). We found that VCA domain expression inhibited actin filopodia induced by Map (Figure 5K). In control experiments, VCA domain expression also blocked filopodia formation induced by active Cdc42V12 (data not shown). However, IpgB2 could stimulate actin stress fiber formation under similar experimental conditions (data not shown), demonstrating that the VCA inhibits specific Arp2/3-mediated events. These data further suggest that Map functions operationally similar to IpgB2 as molecular mimic of GTPases.

## WxxxE Effectors Have Functional Eukaryotic Subcellular Targeting Motifs

We noticed that some WxxxE proteins have putative C-terminal subcellular targeting sequences (Figure 6A, yellow). In fact, the last three residues of Map (-Thr-Arg-Leu-stop) conform to a consensus type I PDZ ligand motif (-Ser/Thr-X-Hydrophobic-stop). To identify binding partners for the putative PDZ ligand in Map, a mouse embryo library was screened by the yeast two-hybrid method. We identified

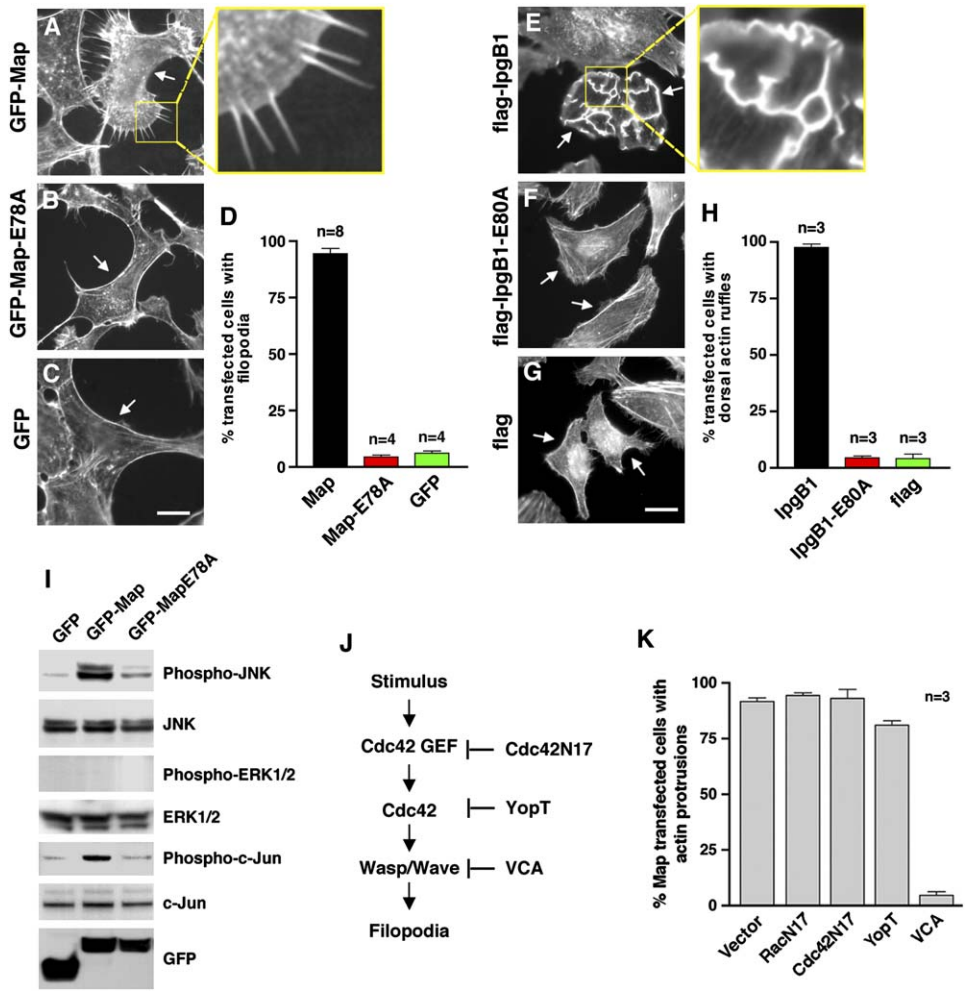


**Figure 5. Map and IpgB1 Induce Filopodia and Lamellipodia, Respectively**

(A–C) Immunofluorescence microscopy of actin in HEK293A cells transfected with GFP-Map (A) GFP-MapE66A (B), or GFP (C). The boxed region is a magnification of Map induced filopodia. Arrows indicate transfected cells. Scale bar, 15 μm.

(D) Quantification of new filopodia in HEK293A cells transfected with plasmids shown in (A)–(C). One hundred fifty transfected cells were counted in at least four independent experiments. Data are presented as mean ±SEM.

(E–G) Immunofluorescence microscopy of actin in HEK293A cells transfected with GFP-IpgB1 (E) GFP-IpgB1-E80A (F), or GFP (G). The boxed region is a magnification of IpgB1 induced lamellipodia. Arrows indicate transfected cells. Scale bar, 15 μm.

(H) Quantification of new lamellipodia in HEK293A cells transfected with plasmids shown in (E) –(G). One hundred fifty transfected cells were counted in three independent experiments. Data are presented as mean ±SEM.

(I) Whole-cell lysates expressing GFP, GFP-Map, or GFP-Map-E78A were immunoblotted with the indicated antibodies (right) by immunoblot.

(J) Diagram showing the concerted Cdc42 signaling pathway and the inhibitors used in Figure 5K.

(K) HEK293A cells were cotransfected with 0.5 μg of GFP-Map and a 3-fold excess (1.5 μg) of the indicated cDNA inhibitors. At least 150 cotransfected cells were scored for localized filopodia in three experimental trials. Data are presented as mean ±SEM.

seven identical clones corresponding to the second PDZ domain of Ezrin binding protein 50 (Ebp50, also known as NHERF1; Figure 6B). Remarkably, C-terminal VQDTRL* sequence is identical to the C terminus of the cystic fibrosis transmembrane regulator (CFTR), a high-affinity Ebp50 binding protein (Figure 6C; Short et al., 1998).

To test this interaction in vitro, a recombinant maltose binding protein (MBP) fusion of either Map or IpgB2 (Figure 6D) was mixed with recombinant [$^{35}$S]-labeled Ebp50 produced in a rabbit reticulocyte in vitro transcription/translation system (Figure 6E). Amylose-Sepharose pull down revealed that Ebp50 directly interacts with Map but not with control IpgB2 (Figure 6F). In addition, endogenous Ebp50 interacted with GFP-Map in co immunoprecipitation experiments, suggesting that Map and Ebp50 form a complex in HEK293A cells (Figure 6G). In contrast, Ebp50 did not bind to mutant MapΔTRL, confirming that this binding occurs through a type I PDZ domain interaction (Figure 6G).

Ebp50 is a component of cell surface microvilli where it functions to target membrane receptors to the apical surface

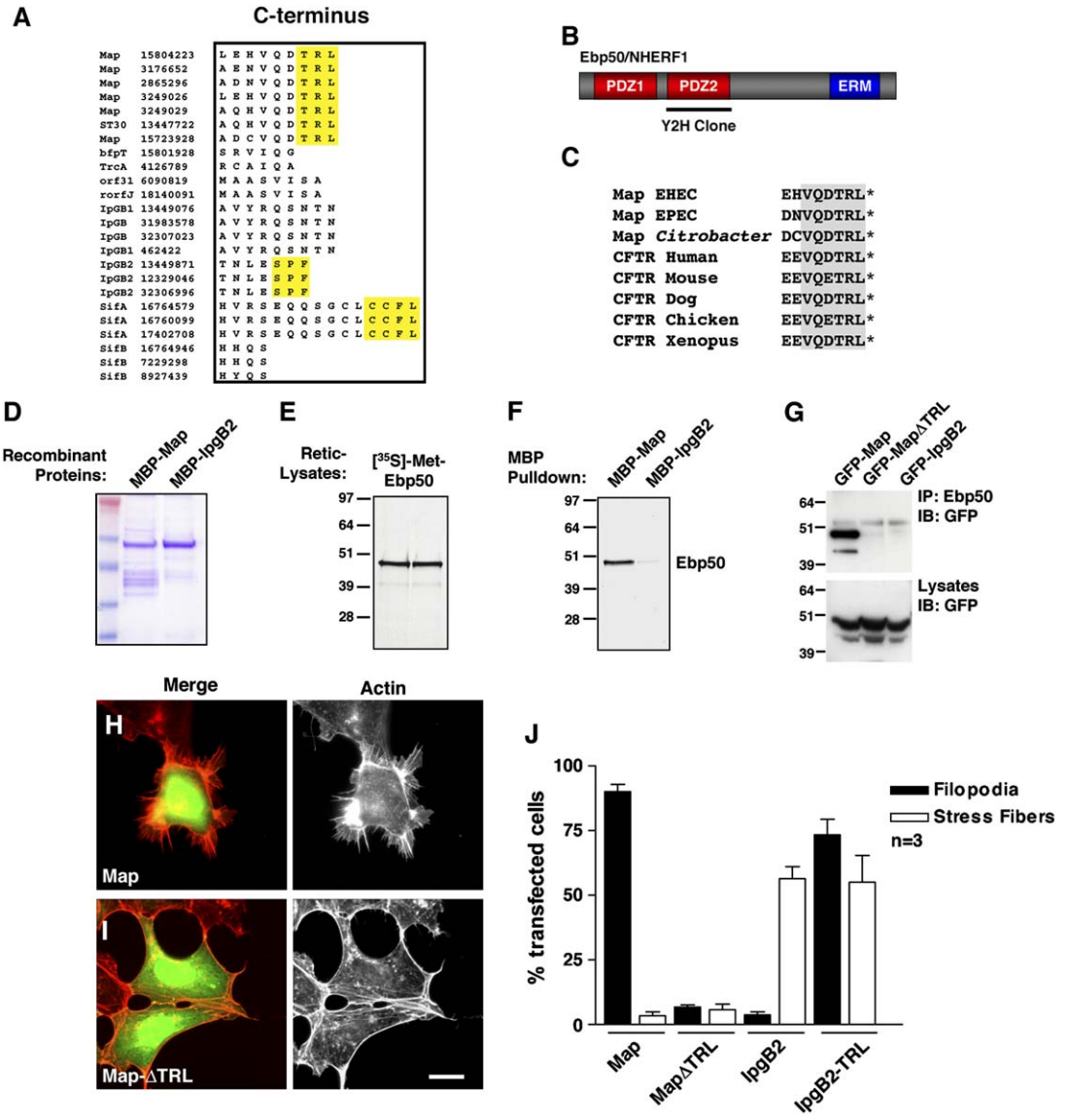


**Figure 6. Map Interacts with Ebp50 through a Conserved PDZ Binding Motif**

(A) C-terminal residues of the WxxxE family shown in Figure 1A. Yellow box indicates either type I PDZ ligand or CaaX box.

(B) Diagram of Ebp50 depicting two PDZ domains and the Ezrin/Radixin/Moesin binding domain (ERM). The specific yeast-two hybrid clone of Ebp50 that interacts with Map is indicated below.

(C) Sequence alignment comparing the C-terminal 8 residues found in Map to those in CFTR. The bacterial or eukaryotic species are indicated.

(D) Coomassie stain of 10 μg of bacterial expressed and purified Map and IpgB2 MBP fusion proteins.

(E) Autoradiograph of 1/20 input of [$^{35}$S]-methionine labeled Ebp50 produced by an in vitro transcription/translation reaction.

(F) Amylose-Sepharose pull down of MBP-Map or MBP-IpgB2 mixed with [$^{35}$S]-met-Ebp50. Autoradiograph is shown.

(G) HEK293A cells were transfected with indicated GFP constructs. Cell lysates were immunoprecipitated with anit-Ebp50 antibody and immunoblotted for GFP (top). Cell lysates were probed anti-GFP immunoblot to show input levels (bottom).

(H and I) Immunfluorescence microscopy HEK293A cells transfected with GFP-Map (H) and GFP-MapΔTRL (I). Actin was detected by rhodamine phalloidin staining and images are shown in gray scale for better contrast (right panels). Scale bar, 15μm.

(J) Quantification of filopodia formation (black bars) or actin stress fibers formation (white bars) in HEK293A cells transfected with the indicated plasmids. At least 150 cells were counted for three independent experiments. Data are presented as mean ±SEM.

of epithelial cells (Bretscher et al., 2000). Thus, Ebp50 may direct Map to the plasma membrane through the PDZ domain interaction. As a functional test of this idea, we observed cell surface filopodia formation in cells expressing the Ebp50 binding-deficient mutant MapΔTRL. Compared to the filopodia induced by wild-type Map (Figure 6H), the actin cytoskeleton in cells expressing MapΔTRL (Figure 6I) was indistinguishable from that of GFP-transfected cells (see

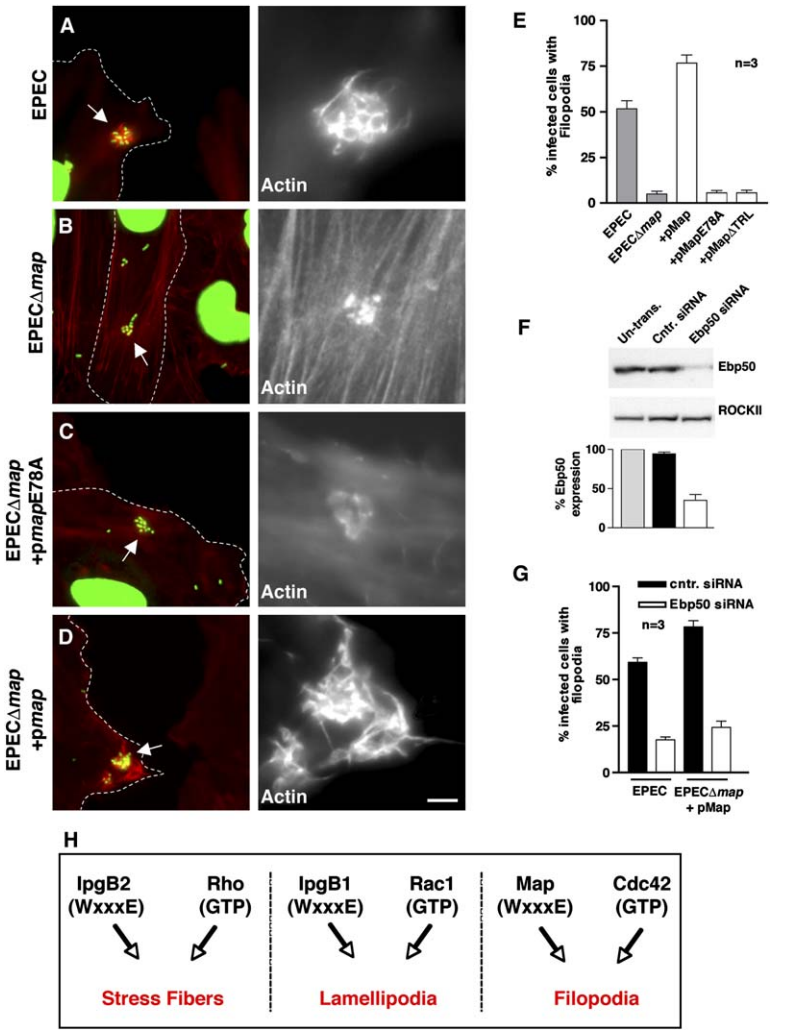


**Figure 7. Functional Characterization of Map during EPEC Pathogenesis**

(A and B) Fluorescence microscopy of HeLa cells infected with EPEC (A) or EPEC$\Delta$*map* (B) for 30 min. Images to the left show HeLa cells stained with rhodamine phalloidin to detect cellular actin (dotted line) and DAPI (green) to detect EPEC microcolonies. Images to the right show a 4× magnification of the area indicated by arrows in the left image. Actin staining is presented in gray scale to help contrast.

(C and D) HeLa cells infected with EPEC$\Delta$*map* strain carrying plasmids encoding MapE78A mutant (C) or wild-type Map (D). Cell images are presented as described in (A) and (B). Scale bar, 5 μm.

(E) Quantification of filopodia formation in HeLa cells infected with EPEC or EPEC$\Delta$*map* (gray bars). In addition, EPEC$\Delta$*map* carrying the indicated plasmids are shown (white bars). At least 50 EPEC infection sites were scored for the formation of filopodia in three independent experiments. Data are presented as mean ±SEM.

(F) Untransfected, control siRNA, or Ebp50 siRNA-transfected cells were subjected to Ebp50 (top) or ROCKII (middle) immunoblot. Average arbitrary densitometry units from Ebp50 Western blots were quantified from three independent experiments (bottom).

(G) HeLa cells were transfected with control siRNA (black bars) or Ebp50 siRNA (white bars). Twenty-four hours later, cells were infected with wild-type EPEC or EPEC$\Delta$*map* + p*map* for 30 min.

(H) Our model postulates that three individual WxxxE effectors, IpgB2, IpgB1, and Map induce three distinct actin phenotypes, stress fibers, cell surface lamellipodia, and filopodia, respectively. Each of these actin phenotypes are induced by the GTP bound form of respective RhoA, Rac1, and Cdc42.

Figure 5C). Quantification of these results are shown in Figure 6J. We asked if subcellular localization could impart signaling specificity to the WxxxE effectors. As noted in Figure 6J, IpgB2-expressing cells display stress fiber formation with an apparent absence of filopodia. We fused the C-terminal PDZ motif (TRL) of Map to the C terminus of IpgB2. Transfection of the IpgB2-TRL chimera resulted in new cell surface filopodia in the majority of cells (Figure 6J). Coimmunoprecipitation experiments confirmed that Ebp50 interacts with the IpgB2-TRL chimera (data not shown). These data suggest that Ebp50 is a critical component of Map signaling and specificity.

## Map Activity as a GTPase Mimic and Subcellular Targeting Are Required for EPEC Pathogenesis

To ensure that our observed phenotypes were not the result of overexpression of Map in cultured cells, we investigated host cell filopodia formation in cells infected with EPEC, a pathogen that naturally expresses Map during infection (Kenny and Jepson, 2000). EPEC infected HeLa cells produced cell surface filopodia that surround the bacterial microcolonies (Figure 7A; Kenny et al., 2002). In contrast, a *map* gene-deletion strain (EPEC$\Delta$*map*) did not induce filopodia in host cells (Figure 7B;Kenny et al., 2002). Next, we introduced expression plasmids carrying the wild-type *map* gene (denoted as p*map*) or a *map* gene harboring a single $E^{78}\rightarrow A$ point mutation (p*map*E78A) into the EPEC$\Delta$*map* strain. While type III delivery of MapE78A failed to induce cell surface filopodia (Figure 7C), the phenotype was recovered by complementing the EPEC$\Delta$*map* with wild-type Map in *trans* (Figure 7D). Quantification of these results are shown in Figure 7E. These data reaffirm the critical role that residues in the WxxxE motif play for proper function of Map during EPEC pathogenesis.

Next, we investigated the physiological relevance of Map targeting to the cell surface through its interaction with host cell Ebp50. First, we expressed plasmid-encoded Map$\Delta$TRL (p*map*$\Delta$TRL) in the EPEC$\Delta$*map* strain. As shown in Figure 7E, type III delivery of Map$\Delta$TRL failed to induce filopodia in HeLa cells. To determine if this result is due to the interaction between Map and Ebp50 we knocked down Ebp50 protein levels by RNA interference. Ebp50 protein

was reduced ~70% by specific siRNA treatment compared to controls (Figure 7F). Application of Ebp50 siRNA to cells 24 hr prior to wild-type EPEC infections significantly reduced the incidence of cellular filopodia formation (Figure 7G). Similar results were found upon infection of the EPEC*Δmap* + p*map* strain (Figure 7G). These data further demonstrate that intracellular targeting by host cell Ebp50 is required for proper Map function during bacterial pathogenesis.

## DISCUSSION

In this study, we have used the *Shigella* effector IpgB1 and IpgB2 as well as the *E. coli* effector Map as experimental prototypes to demonstrate that several WxxxE family members functionally mimic the activated forms of distinct Rho family small G proteins (Figure 7H). These results further highlight the remarkable ability of bacterial effectors to subvert small G protein signaling pathways through molecular mimicry of eukaryotic proteins (Stebbins and Galan, 2001).

### WxxxE Effectors Are Functional Mimics of Mammalian Small G Protein

Multiple lines of evidence support our GTPase mimicry postulate. First, three individual WxxxE effectors, IpgB1, IpgB2, and Map induce three distinct phenotypes, dorsal ruffles, stress fibers, and filopodia that normally result from activation of Rac1, RhoA, and Cdc42, respectively. Whereas IpgB2 and Map maintained the ability to induce actin cytoskeletal changes in the absence of Rho family GTPases, inhibition of downstream GTPase signaling pathways abolished the activity of these bacterial effectors. Consistent with these observations, we found that IpgB2 interacted with the GBD regions of several natural RhoA ligands. Interestingly, the biological effects of IpgB2 are not restricted to mammalian cells; PGA analysis suggests that IpgB2 induced yeast cell death by overstimulating the Pkc1p Rho-kinase signal transduction pathway. In fact, the gene transcription profiles induced by IpgB2 compares favorably to that of GTP bound Rho1p. Finally, we confirmed the role of Map as a physiological mimic of GTPases with a series of EPEC infection studies. Thus, our studies provide evidence in support of a GTPase-independent mechanism for the induction of critical actin dynamic events.

We aligned our effector protein family using the invariant WxxxE motif as a molecular signature of functionality. This initial criterion was proven correct as mutations in the invariant Trp or Glu residues inhibited the GTPase mimicry activity of IpgB1, IpgB2, and Map. These effector proteins appear to be a bacterial ''invention'' since there are no WxxxE motifs in eukaryotic small G proteins and IpgB1, IpgB2, nor Map bind guanine nucleotides or display sequences, suggesting that they have GTPase activity. It is unlikely that two invariant residues could impart this remarkable signaling specificity. We imagine that the sequences surrounding the WxxxE motif may also contribute to binding and induce a conformational switch in GBD-containing target proteins. This scenario would be analogous to the mechanisms that have been proposed for GTP bound small G proteins affecting their downstream targets (Lei et al., 2000). Since this is only speculation, additional structural data showing WxxxE effectors bound to their downstream target proteins should provide insights into the molecular mechanisms of GTPase mimicry.

### Does Our Model Fit with the Known Properties of Other WxxxE Effectors?

Based on the function of IpgB1, IpgB2, and Map it may be possible to infer the activities of additional WxxxE family members. In light of this information, we now recognize that the *Salmonella* effector SifA displays cell-signaling characteristics analogous to members of the Rab subfamily of small G proteins. For instance, SifA has been suggested to regulate membrane trafficking to the intracellular vacuole that houses *Salmonella* in the host cell cytoplasm (Beuzon et al., 2000). In addition, SifA plays a role in extending the *Salmonella*-inducible filament (Sif) membrane networks along the microtubule cytoskeleton (Beuzon et al., 2000; Brumell et al., 2002; Stein et al., 1996). Consistent with this observation, a recent report demonstrates that SifA recruits kinesin motor proteins to the Sif membranes through the adaptor protein SifA-kinesin-interacting protein (SKIP; Boucrot et al., 2005). Similarly, Rab GTPases direct membrane fusion events and are required for membrane trafficking along cytoskeletal networks by coupling motor proteins to cognate membranes. Thus, the biological function of SifA is in agreement with our hypothesis that effectors from this family are likely to possess GTPase mimicry capabilities.

### Guided Missiles: Localizing WxxxE Effectors Determine Their Signaling Specificity

Several of the WxxxE effectors have evolved sequences that serve as localization determinants in the host cell. For example, we identified a functional eukaryotic PDZ ligand at the C terminus of Map. Remarkably, VQDTRL sequence is identical to the well-characterized PDZ ligand found in eukaryotic CFTR. Consistent with this finding, both Map and CFTR interact with the adaptor protein Ebp50 through a PDZ/ligand interaction. Although this is only speculation, the PDZ motif of Map most likely acts as an apical membrane retention sequence since Ebp50 is highly enriched in this cellular compartment and this is the site of enteric *E. coli* type III secretion. Because bacterial effectors are injected at low concentrations, specific eukaryotic targeting sequences could direct these effectors to specific sites within the host cell. Future experimentation will be aimed at understanding the physiological role of Map as a functional mimic of GTPases at the apical surface of intestinal epithelial cells.

Interestingly, eukaryotic targeting sequences seem to be common among the WxxxE effector family. For example, SifA also possesses a functional C-terminal targeting motif that is quite similar to the C-terminal CaaX box found in many eukaryotic small G proteins (Figure 6A, yellow; Boucrot et al., 2003). In fact, this CaaX motif is required for targeting SifA to newly forming *Salmonella* inducible filaments, a process that is necessary for its proper signaling function (Boucrot et al., 2003). Therefore, at least two WxxxE family

members, Map and SifA, have evolved functional C-terminal targeting motifs that are used by eukaryotic proteins. We expect other WxxxE effector will be localized to specific host cell compartments through yet-to-be-identified targeting sequences.

## Pathogenic Genetic Array: Using Yeast to Study Bacterial Effector Proteins

Yeast can serve as an excellent model organism to study bacterial effector protein functions (Lesser and Miller, 2001). We have describing two high-throughput genome-screening procedures used to elucidate the functions of specific effectors that are toxic to yeast. The PGA screen illustrated in Figure 3B was designed based on previously described synthetic lethality screens and the SGA screen (Tong et al., 2001). In addition, we used DNA microarray expression profiling as a second method to analyze the role of IpgB2 in yeast. Although we used these genome screening procedures as an unbiased conformation of our mammalian cell biology data, the PGA screen, and DNA microarray profiling may serve as useful tools to help identify the functions of other pathogen effector proteins or toxins that target-specific substrates in yeast.

## Conclusion

Our studies suggest for the first time that IpgB1, IpgB2, and Map function by a common molecular mechanism as functional mimics of distinct Rho family GTPases. As shown in Figure 7H, IpgB2 induces actin stress fibers, IpgB1 induces dorsal lamellipodia, and Map induces cell surface filopodia. The respective GTPases RhoA, Rac1, and Cdc42 share these phenotypes. Future studies should reveal the actions of additional WxxxE effectors, findings that may provide important new insights into both eukaryotic small G protein signaling pathways and bacterial pathogenic mechanisms.

## EXPERIMENTAL PROCEDURES

### Plasmids and siRNA

The *map* gene (accession # AP002566) was cloned from EHEC O157:H7 genomic DNA, and the *ipgb1* (CAA33379) or *ipgb2* gene (AF348706) were cloned from *Shigella flexneri* pWR100 virulence plasmid (ATCC) by PCR. Map and IpgB2 were cloned in frame into pEGFP-C2 (Clontech) and IpgB1 was cloned into FLAG-tagged pcDNA3.1 following standard protocols. All GTPase constructs were purchased from the Guthrie Institute. Dr. Jeffrey Frost provided pEF-C3 exoenzyme. ROCKI and mDia1 cDNAs were provided Dr. Shuh Narumiya. For expression in yeast, *ipgb2* was cloned into pYes-DEST52 (*Gal1* promoter) using Gateway technology (Invitrogen). For bacterial complementation, the EHEC *map* gene was subcloned down stream of the *lacZ* promoter in pBBR1MCS1, a plasmid that replicates autonomously in *E. coli*. All point mutations were generated with the QuickChange Site-Directed Mutagenesis kit (Stratagene) following manufacturer's instructions. All constructs were verified by DNA sequencing. Ebp50 siRNA sequence (5′-GGAGAACAGUCGU GAAGCCtt) or control siRNA were purchased from Ambion.

### Cell Culture, Transfection, siRNA, Immunocytochemistry, and Fluorescence Microscopy

HEK293A cells were maintained as previously described (Shao et al., 2002). Transfections were performed using FuGENE 6 (Roche). siRNA tranfections were performed using siPORT amine (Ambion). To assess cell morphology, cells were seeded on fibronectin-coated coverslips (BD Bioscience) and cultured overnight in 6-well dishes. Cells were transfected for 16–20 hr, fixed and processed for immunocytochemistry. Immunofuorescence microscopy was performed on a Zeiss Axiovert 200M microscope using the appropriate filter sets and Metafluor software.

### Immunoprecipitation, Immunoblotting, and Antibodies

Transfections were performed for 16–24 hr, followed by lysis in IP buffer (20 mM Tris-HCl [pH 7.4], 150 mM NaCl, 1 mM EDTA, 1% Triton X-100, and protease inhibitor cocktail Roche]). Recombinant proteins were immunoprecipitated using protein A Sepharose (Invitrogen)-conjugated primary antibodies. Anti-GFP polyclonal and monoclonal (Clontech), anti-myc 9E10 (Roche), anti-FLAG M2, anti-FLAG polyclonal, and anti-HA (Covance) were used for immunoblotting.

### ROCK Kinase Assay

Ten centimeter dishes of HEK293A cells were transfected with myc-ROCKI and GFP-IpGB2, GFP-Map, or GFP alone. Anti-GFP immunoprecipitated proteins were washed with IP buffer followed by extensive washes in kinase buffer (20 mM Tris-HCl [pH 7.4], 10 mM $MgCl_2$, 1 mg/ml BSA, 1 mM DTT). Samples were resuspended in 200 μl kinase buffer and split into two samples, one was left untreated and the other was incubated for 15 min at 4ºC with Y27632 (10 μM). The second set of samples contained no inhibitor. 1μCi [$^{32}$P]-ATP and 1 μM S6 peptide (QIAKRRRLSSLRA, single amino acid code) were added to the reaction mix and placed at 30ºC. Ten microliter samples were removed at given time points and spotted on p81 Whatman paper. Samples were washed six times in 80 mM phosphoric acid, dried, and Cherenkov units were counted. Data was graphed using Prism software.

### Yeast Two-Hybrid and Yeast Toxicity Assays

Yeast two-hybrid experiments were performed as described previously (Hollenberg et al., 1995). All yeast transformations were carried out by standard lithium acetate method. Approximately six million clones were screened by IpgB2-E66A and ~10 million clones were screened by Map. For yeast toxicity assays, *Saccharomyces cerevisiae* (strain INVsc1, Invitrogen) were grown on minimal medium + 2% glucose to repress *GAL1-IpgB2* expression. Expression of *GAL1-IpgB2* or mutants was induced by plating yeast on medium with 2% galactose as the carbon source. For all assays, transformed yeast colonies were incubated at 30ºC for 48 hr.

### Pathogenic Genetic Array

*GAL1-IpgB2* was introduced in the yeast strain Y7092 (*MATα can1Δ::STE2pr-SpΔhis5 his3Δ1 leu2Δ0 ura3Δ0 met15Δ0 lyp1Δ trp1Δ::GAL1-IpgB1-URA3*). Briefly, *GAL1-IpgB2* was PCR amplified and the PCR product contained 55 nucleotides of the *trp1* gene at the 5′ end and a 25 bp unique region at the 3′ end. A second PCR amplification produced the *ura3* gene containing the corresponding 25 bp unique region at the 5′ end and the terminal 55 bp of the *trp1* gene at the 3′ end. Both PCR products were transformed into Y7092, and recombinants were selected on minimal medium minus uracil. The PGA analysis was conducted using the SGA methodology, as described in Tong et al. (2001) with the following modifications: double-mutant meiotic progeny were selected on medium containing glucose, moved to medium containing raffinose, then transferred to and scored on galactose medium.

### Yeast DNA Microarray

Strains containing the following expression plasmids, *GAL1*-driven *IpgB2*, *RHO1-Q68H*, *PKC1-R398A*, and *STE4* (R. Sopko and B. Andrews) were induced in 2% galactose for 3 hr. Preparation of samples for hybridization to microarrays, image acquisition, and data analyses were carried out as previously described (Grigull et al., 2004). Pearson correlations of microarray data from paired combinations of experiments were determined using Excel software.

### Bacterial Infections and Complementation

HeLa cells were infected for 30 min with preactivated EPEC as described previously (Kenny et al., 2002). Complementation plasmid pBBR1MCS1 carrying the EHEC *map, mapE78A,* or *mapΔTRL* gene was introduced into EPEC*Δmap* strain (B. Kenny) using triparental mating procedure with the mobilization plasmid pRK2013.

### Supplemental Data

Supplemental Data include one figure and can be found with this article online at http://www.cell.com/cgi/content/full/124/1/133/DC1/.

## ACKNOWLEDGMENTS

We would like to thank D. Friedberg, L. Bertelsen, K. Barrett, and all members of the Dixon Lab for fruitful discussions in preparation of this manuscript. We are grateful to B. Kenny, S. Narumiya, J. Frost, R. Sopko, and B. Andrews for providing invaluable reagents. Grants from the NIH, the Walther Cancer Institute, and the Ellison Foundation supported this research (J.E.D.). N.M.A. and S.M. are supported by the Hematology and Diabetes NIH training grants. Grants from CIHR, Genome Canada, and Genome Ontario support C.B. and T.R.H.

Received: July 22, 2005
Revised: September 8, 2005
Accepted: October 18, 2005
Published: January 12, 2006

## REFERENCES

Aktories, K., Wilde, C., and Vogelsgesang, M. (2004). Rho-modifying C3-like ADP-ribosyltransferases. Rev. Physiol. Biochem. Pharmacol. *152*, 1–22.

Amano, M., Chihara, K., Kimura, K., Fukata, Y., Nakamura, N., Matsuura, Y., and Kaibuchi, K. (1997). Formation of actin stress fibers and focal adhesions enhanced by Rho-kinase. Science *275*, 1308–1311.

Beuzon, C.R., Meresse, S., Unsworth, K.E., Ruiz-Albert, J., Garvis, S., Waterman, S.R., Ryder, T.A., Boucrot, E., and Holden, D.W. (2000). Salmonella maintains the integrity of its intracellular vacuole through the action of SifA. EMBO J. *19*, 3235–3249.

Boquet, P. (2000). Small GTP binding proteins and bacterial virulence. Microbes Infect. *2*, 837–843.

Boucrot, E., Beuzon, C.R., Holden, D.W., Gorvel, J.P., and Meresse, S. (2003). Salmonella typhimurium SifA effector protein requires its membrane-anchoring C-terminal hexapeptide for its biological function. J. Biol. Chem. *278*, 14196–14202.

Boucrot, E., Henry, T., Borg, J.P., Gorvel, J.P., and Meresse, S. (2005). The intracellular fate of Salmonella depends on the recruitment of kinesin. Science *308*, 1174–1178.

Bretscher, A., Chambers, D., Nguyen, R., and Reczek, D. (2000). ERM-Merlin and EBP50 protein families in plasma membrane organization and function. Annu. Rev. Cell Dev. Biol. *16*, 113–143.

Brumell, J.H., Goosney, D.L., and Finlay, B.B. (2002). SifA, a type III secreted effector of Salmonella typhimurium, directs Salmonella-induced filament (Sif) formation along microtubules. Traffic *3*, 407–415.

Cornelis, G.R., and Van Gijsegem, F. (2000). Assembly and function of type III secretory systems. Annu. Rev. Microbiol. *54*, 735–774.

Cossart, P., and Sansonetti, P.J. (2004). Bacterial invasion: the paradigms of enteroinvasive pathogens. Science *304*, 242–248.

Dean, P., and Kenny, B. (2004). Intestinal barrier dysfunction by enteropathogenic Escherichia coli is mediated by two effector molecules and a bacterial surface protein. Mol. Microbiol. *54*, 665–675.

Dean, P., Maresca, M., and Kenny, B. (2005). EPEC's weapons of mass subversion. Curr. Opin. Microbiol. *8*, 28–34.

Galan, J.E., and Collmer, A. (1999). Type III secretion machines: bacterial devices for protein delivery into host cells. Science *284*, 1322–1328.

Grigull, J., Mnaimneh, S., Pootoolal, J., Robinson, M.D., and Hughes, T.R. (2004). Genome-wide analysis of mRNA stability using transcription inhibitors and microarrays reveals posttranscriptional control of ribosome biogenesis factors. Mol. Cell. Biol. *24*, 5534–5547.

Heinisch, J.J., Lorberg, A., Schmitz, H.P., and Jacoby, J.J. (1999). The protein kinase C-mediated MAP kinase pathway involved in the maintenance of cellular integrity in Saccharomyces cerevisiae. Mol. Microbiol. *32*, 671–680.

Hollenberg, S.M., Sternglanz, R., Cheng, P.F., and Weintraub, H. (1995). Identification of a new family of tissue-specific basic helix-loop-helix proteins with a two-hybrid system. Mol. Cell. Biol. *15*, 3813–3822.

Iriarte, M., and Cornelis, G.R. (1998). YopT, a new Yersinia Yop effector protein, affects the cytoskeleton of host cells. Mol. Microbiol. *29*, 915–929.

Jung, U.S., and Levin, D.E. (1999). Genome-wide analysis of gene expression regulated by the yeast cell wall integrity signalling pathway. Mol. Microbiol. *34*, 1049–1057.

Kenny, B., and Jepson, M. (2000). Targeting of an enteropathogenic Escherichia coli (EPEC) effector protein to host mitochondria. Cell. Microbiol. *2*, 579–590.

Kenny, B., Ellis, S., Leard, A.D., Warawa, J., Mellor, H., and Jepson, M.A. (2002). Co-ordinate regulation of distinct host cell signalling pathways by multifunctional enteropathogenic Escherichia coli effector molecules. Mol. Microbiol. *44*, 1095–1107.

Lei, M., Lu, W., Meng, W., Parrini, M.C., Eck, M.J., Mayer, B.J., and Harrison, S.C. (2000). Structure of PAK1 in an autoinhibited conformation reveals a multistage activation switch. Cell *102*, 387–397.

Lesser, C.F., and Miller, S.I. (2001). Expression of microbial virulence proteins in Saccharomyces cerevisiae models mammalian infection. EMBO J. *20*, 1840–1849.

Machesky, L.M., and Insall, R.H. (1998). Scar1 and the related Wiskott-Aldrich syndrome protein, WASP, regulate the actin cytoskeleton through the Arp2/3 complex. Curr. Biol. *8*, 1347–1356.

Madaule, P., Furuyashiki, T., Reid, T., Ishizaki, T., Watanabe, G., Morii, N., and Narumiya, S. (1995). A novel partner for the GTP-bound forms of rho and rac. FEBS Lett. *377*, 243–248.

Mundy, R., Petrovska, L., Smollett, K., Simpson, N., Wilson, R.K., Yu, J., Tu, X., Rosenshine, I., Clare, S., Dougan, G., and Frankel, G. (2004). Identification of a novel Citrobacter rodentium type III secreted protein, EspI, and roles of this and other secreted proteins in infection. Infect. Immun. *72*, 2288–2302.

Nobes, C.D., and Hall, A. (1995). Rho, rac, and cdc42 GTPases regulate the assembly of multimolecular focal complexes associated with actin stress fibers, lamellipodia, and filopodia. Cell *81*, 53–62.

Ohya, K., Handa, Y., Ogawa, M., Suzuki, M., and Sasakawa, C. (2005). IpgB1 is a novel Shigella effector protein involved in bacterial invasion of host cells: its activity to promote membrane ruffling via RAC1 and CDC42 activation. J. Biol. Chem. *280*, 24022–24034.

Ridley, A.J., and Hall, A. (1992). The small GTP-binding protein rho regulates the assembly of focal adhesions and actin stress fibers in response to growth factors. Cell *70*, 389–399.

Roberts, C.J., Nelson, B., Marton, M.J., Stoughton, R., Meyer, M.R., Bennett, H.A., He, Y.D., Dai, H., Walker, W.L., Hughes, T.R., et al. (2000). Signaling and circuitry of multiple MAPK pathways revealed by a matrix of global gene expression profiles. Science *287*, 873–880.

Shao, F., Merritt, P.M., Bao, Z., Innes, R.W., and Dixon, J.E. (2002). A Yersinia effector and a Pseudomonas avirulence protein define a family of cysteine proteases functioning in bacterial pathogenesis. Cell *109*, 575–588.

Short, D.B., Trotter, K.W., Reczek, D., Kreda, S.M., Bretscher, A., Boucher, R.C., Stutts, M.J., and Milgram, S.L. (1998). An apical PDZ protein anchors the cystic fibrosis transmembrane conductance regulator to the cytoskeleton. J. Biol. Chem. *273*, 19797–19801.

Stebbins, C.E., and Galan, J.E. (2001). Structural mimicry in bacterial virulence. Nature *412*, 701–705.

Stein, M.A., Leung, K.Y., Zwick, M., Garcia-del Portillo, F., and Finlay, B.B. (1996). Identification of a Salmonella virulence gene required for formation of filamentous structures containing lysosomal membrane glycoproteins within epithelial cells. Mol. Microbiol. *20*, 151–164.

Tong, A.H., Evangelista, M., Parsons, A.B., Xu, H., Bader, G.D., Page, N., Robinson, M., Raghibizadeh, S., Hogue, C.W., Bussey, H., et al. (2001). Systematic genetic analysis with ordered arrays of yeast deletion mutants. Science *294*, 2364–2368.

Watanabe, N., Kato, T., Fujita, A., Ishizaki, T., and Narumiya, S. (1999). Cooperation between mDia1 and ROCK in Rho-induced actin reorganization. Nat. Cell Biol. *1*, 136–143.

Whiteway, M., Hougan, L., and Thomas, D.Y. (1990). Overexpression of the STE4 gene leads to mating response in haploid Saccharomyces cerevisiae. Mol. Cell. Biol. *10*, 217–222.